Geophysical Research Letters

RESEARCH LETTER
10.1029/2020GL088020

Disproving the Bodélé Depression as the Primary Source of Dust Fertilizing the Amazon Rainforest

Yan Yu[1,2], Olga V. Kalashnikova[3], Michael J. Garay[3], Huikyo Lee[3], Michael Notaro[4], James R. Campbell[5], Jared Marquis[6], Paul Ginoux[7], and Gregory S. Okin[1]

[1]Department of Geography, University of California, Los Angeles, CA, USA, [2]Now at Atmospheric and Oceanic Sciences Program, Princeton University, Princeton, NJ, USA, [3]Jet Propulsion Laboratory, California Institute of Technology, Pasadena, CA, USA, [4]Nelson Institute Center for Climatic Research, University of Wisconsin-Madison, Madison, WI, USA, [5]Naval Research Laboratory, Monterey, CA, USA, [6]Department of Atmospheric Sciences, University of North Dakota, Grand Forks, ND, USA, [7]Geophysical Fluid Dynamics Laboratory, National Oceanic and Atmospheric Administration, Princeton, NJ, USA

Key Points:
- The current trajectory simulations quantify observation-derived dust deposition and capture the observed three-dimensional dust distribution
- El Djouf is the preferred source of the transatlantic dust transport, due to favorable transport pathways with respect to seasonal rain belts
- Extensive near-source dust deposition supports the observed limited potential for long-range transport of dust from the Bodélé depression

Supporting Information:
- Supporting Information S1

Correspondence to:
Y. Yu,
yuyan06@gmail.com

Citation:
Yu, Y., Kalashnikova, O. V., Garay, M. J., Lee, H., Notaro, M., Campbell, J. R., et al. (2020). Disproving the Bodélé depression as the primary source of dust fertilizing the Amazon Rainforest. *Geophysical Research Letters*, *47*, e2020GL088020. https://doi.org/10.1029/2020GL088020

Received 20 MAR 2020
Accepted 12 JUN 2020
Accepted article online 20 JUN 2020

Abstract Motivated by the ongoing debates about the relative contribution of specific North African dust sources to the transatlantic dust transport to the Amazon Basin, the current study integrates a suite of satellite observations into a novel trajectory analysis framework to investigate dust transport from the leading two North African dust sources, namely, the Bodélé depression and El Djouf. In particular, this approach provides observation-constrained quantification of the dust's dry and wet deposition along its transport pathways and is validated against multiple satellite observations. The current large ensemble trajectory simulations identify favorable transport pathways from the El Djouf across the Atlantic Ocean with respect to seasonal rain belts. The limited potential for long-range transport of dust from the Bodélé depression is attributed to the currently identified extensive near-source dust removal primarily by dry and wet deposition during boreal winter and summer, respectively.

Plain Language Summary North African deserts have been reported to export ~200 million tons of dust per year to the tropical Atlantic Ocean, degrading air quality over the Caribbean Islands in boreal summer and supplying nutrients to fertilize the Amazon Rainforest in boreal winter and spring through transatlantic dust transport. It has been assumed that the Bodélé depression is the main contributor to this transatlantic dust transport and Amazonian dust fertilization in boreal winter. However, these claims have not been supported by geochemical analysis. Here, we integrate a suite of satellite observations into a novel trajectory analysis framework to investigate dust transport from the leading two North African dust sources, namely, the Bodélé depression and El Djouf, and provide the first ever observation-constrained quantification of the dust's dry and wet deposition along its transport pathways. The approach yields the novel observational finding that the El Djouf is the preferred source of intercontinental transport across the Atlantic Ocean rather than the Bodélé depression, bridging the geochemical impact of North African minerals on the Amazon Basin to the specific dust origin.

1. Introduction

In situ measurements and satellite observations reveal episodes of transatlantic dust transport from North Africa to the Caribbean Islands during boreal summer (Prospero, 1999; Prospero & Lamb, 2003; Prospero & Mayol-Bracero, 2013) and the Amazon Basin during boreal winter to spring (Ben-Ami et al., 2010; Kaufman et al., 2005; Koren et al., 2006; Prospero et al., 1981; Swap et al., 1992; H. Yu, Chin, Yuan, et al., 2015). Based on dust fluxes derived from multiple satellite observations, an estimated 136–222 Tg yr^{-1} of North African dust is deposited over the tropical Atlantic Ocean (H. H. Yu, Tan, et al., 2019), and 8–48 Tg yr^{-1} is deposited into the Amazon Basin (H. Yu, Chin, Yuan, et al., 2015). The transatlantic dust transport exhibits distinct seasonal characteristics in the vertical distribution of transported dust over the tropical Atlantic Ocean, especially the height of the Saharan Air Layer (SAL)—an elevated layer that carries airborne dust during its westward transport across the tropical Atlantic Ocean (Adams et al., 2012; Ben-Ami et al., 2009). In addition, wintertime dust transport to the Amazon Basin (Abouchami et al., 2013) and summertime dust

transport to the Caribbean Islands (Pourmand et al., 2014) are attributed to different active dust sources in North Africa.

In particular, North African dust provides critical phosphorus to fertilize the Amazon Rainforest during its growing season of boreal winter and spring (H. Yu, Chin, Yuan, et al., 2015). Due to substantial leaching and the resulting deficiency of phosphorus in Amazonian soils, the long-term productivity of the Amazon Rainforest largely depends on this imported dust (Okin et al., 2004). Based on chemical analysis and an atmospheric model, Barkley et al. (2019) estimated about 0.011–0.033 Tg yr^{-1} of phosphorus is transported associated with African dust into the Amazon Basin.

The quantitative influence of North African dust on maintaining the productivity of the Amazon Rainforest in boreal winter and spring remains largely uncertain (H. Yu, Chin, Yuan, et al., 2015) due to the disparity in measured chemical composition based on the specific North African dust sources and their unclear contribution to the Amazon Basin (Bristow et al., 2010; Hudson-Edwards et al., 2014; Okin et al., 2004). Based on dust flux calculations derived from aerosol optical depth (AOD) observed by the Moderate Resolution Imaging Spectroradiometer (MODIS), Koren et al. (2006) first hypothesized that more than half of this dust in boreal winter originates from the Bodélé depression, the leading global dust source (Crouvi et al., 2012; Evan et al., 2016; Ginoux et al., 2010, 2012; Schepanski et al., 2012; Washington et al., 2006; Y. Yu et al., 2018). However, this hypothesis was dependent on several untested assumptions about the spatial distribution of dust deposition, such as homogeneous deposition rate over the downwind region. Furthermore, the hypothesized dominant contribution from the Bodélé depression to transatlantic dust transport to South America in boreal winter and spring has proven inconsistent with surface sediment and geochemical analysis in Amazonia (Abouchami et al., 2013). Global chemistry transport models (CTMs) have been widely used for studying dust transport from North Africa (Gläser et al., 2015; Ridley et al., 2012; Wang et al., 2016). The credibility of CTM-based results, however, is largely limited by the uncertainty in these models' highly parameterized dust emission and deposition processes (Ridley et al., 2013). For example, the Goddard Chemistry Aerosol Radiation and Transport (GOCART) model, a widely used CTM, overestimates dust deposition rates during transatlantic transport, suggested by substantial lower dust optical depth (DOD) over the tropical Atlantic Ocean simulated by the model compared with satellite observations (D. Kim et al., 2017). Therefore, observational characterization of the climatology of transatlantic dust transport is critically needed for testing the satellite-based hypothesis regarding the specific dominant North African dust source influencing the Amazon Rainforest in boreal winter to spring. Inspired by evidences suggesting that the leading contribution of Western African deserts to the tropical Atlantic from both geochemical analyses (Bozlaker et al., 2018; Kumar et al., 2018; Pourmand et al., 2014) and modeling work (Ridley et al., 2012; Wang et al., 2016), we raise an alternative hypothesis that the West African deserts contribute more dust than the Bodélé depression to the Amazon Basin in boreal winter.

Motivated by the aforementioned needs and challenges in the observational quantification of North African dust transported to the Amazon Basin from specific dust sources, we investigate the transatlantic dust transport from the leading two North African dust sources, namely, the Bodélé depression (in Chad) and West African El Djouf (in Mauritania and Mali), by applying a observationally constrained trajectory analysis framework. The applied trajectory model initiates millions of dust particles with an effective plume height observed by the Multiangle Imaging SpectroRadiometer (MISR) instrument (Diner et al., 1998; Moroney et al., 2002) on the polar-orbiting Terra satellite. Furthermore, the trajectory model incorporates, and quantifies the impacts of, both dry and wet deposition processes using a suite of satellite observations. The inclusion of dry and wet deposition processes in the trajectory modeling enables a realistic simulation of the three-dimensional atmospheric distribution of transported dust and provides an observation-constrained benchmark for testing the assumptions made by previous satellite-based investigations of transatlantic dust transport (Kaufman et al., 2005; Koren et al., 2006; H. Yu, Tan, et al., 2019; H. Yu, Chin, Bian, et al., 2015; H. Yu, Chin, Yuan, et al., 2015). Based on the observation-constrained trajectory analysis, especially the quantification of dry and wet deposition, the current study tests the contradicting hypotheses regarding the relative contribution of the Bodélé depression and El Djouf to transported dust over the Amazon Basin in boreal winter and spring. We also perform the analysis for boreal summer while reporting the results here for comparison with geochemical and modeling studies.

2. Data and Methods

2.1. MISR Dust Plume Observations

In light of the recently revealed sensitivity of dust transport potential to the injection height of the dust particle (Y. Yu, Kalashnikova, et al., 2019), the current study's trajectory analysis improves upon prior efforts by initiating forward dust trajectories with observed dust plume information. Dust plume top height and motion speed over the Bodélé depression (15–18°N, 12–18°E) and El Djouf (18–22°N, 10–3°W) are obtained from Version F02_0002 of the MISR Level 3 Cloud Motion Vector Product (CMVP) for the period of 2005–2017. In CMVP, imagery from multiple MISR cameras is used to simultaneously retrieve motion (wind speed and direction) and top height of automatically tracked features, such as dust plumes over deserts with mostly clear skies, at a spatial resolution of 17.6 km (Moroney et al., 2002). Following the MISR CMVP-based dust source identification approach (Y. Yu et al., 2018), the study focuses on dust plume data points with reported heights within 2 km of the ground (below boundary layer clouds) and motion speed above 10 m s^{-1}, which is the typical minimum near-surface wind speed required to activate dust emissions across the North Africa and Middle East (Chomette et al., 1999; Menut, 2008). Although 2 km above the ground is lower than the typical SAL height in boreal summer (Adams et al., 2012; Ben-Ami et al., 2009), this conservative threshold minimizes the potential contamination from clouds in the current assessment of dust transport.

2.2. Observationally Constrained Trajectory Modeling

In order to identify and compare the dust transport and spread from both the Bodélé depression and El Djouf, the Hybrid Single-Particle Lagrangian Integrated Trajectory (HYSPLIT) (Stein et al., 2015) model from the National Ocean and Atmosphere Administration (NOAA) Air Resource Laboratory is applied. HYSPLIT-based forward trajectory analysis has been widely used for tracing the downwind evolution of Saharan dust (Salvador et al., 2014). Here, 14-day forward trajectories from both of the North African dust source regions during 2005–2017 are computed based on hourly, three-dimensional wind fields on a 1° × 1° grid from the National Centers for Environmental Prediction (NCEP) Global Data Assimilation System (GDAS). The choice of the 14-day forward trajectories follows the previously estimated typical dust travel time from North Africa to the Americas (Ridley et al., 2012). Although the performance of 2-week forward trajectory analysis over the remote oceans remains uncertain, this uncertainty is partly accounted for in the present study by including dry and wet deposition that usually terminates the forward trajectories earlier than 14 days, as introduced later this section.

The initial date, time (around 10 a.m. local time), latitude, longitude, and height are obtained from MISR CMVP dust plume observations. At each dust plume observation data point, 100 particles are initiated with their initial height randomly chosen from a uniform distribution between the ground to the dust plume top height specified by the MISR CMVP. Corresponding to the available MISR CMVP observations, a total of 1,918,800 forward trajectories is initiated from the Bodélé depression, with 1,227,800 trajectories on 352 days in January–March (JFM) and 691,000 trajectories on 400 days in June–August (JJA) during 2005–2017. A total of 3,234,300 forward trajectories is initiated from the El Djouf, with 1,818,200 trajectories on 424 days in JFM and 1,416,100 trajectories on 456 days in JJA during 2005–2017. The larger number of trajectories initiated from both North African sources in boreal winter is a result of the seasonally enhanced dust activation in both regions (Y. Yu et al., 2018). The uncertainty in the trajectory-based estimates of dust mass loading or deposition over each basin, namely, the tropical Atlantic Ocean, Caribbean Sea, and Amazon Basin, is estimated by subsampling 50% of the trajectories for 10,000 times. The 10th and 90th percentiles of the resulting 10,000 deposition amount values are reported in section 3.2 and supporting information Table S1.

Dry deposition from gravitational settling is considered in the forward trajectory modeling, following the approach taken by advanced dust models (Ginoux et al., 2001; Zender, 2003). During each 1-hr time step of any trajectory, the dust particle is assumed to reach its terminal velocity immediately and settle gravitationally at this velocity. At the end of each 1-hr trajectory time step, the actual particle height is calculated by subtracting the gravitational settling distance from the simulated height from HYSPLIT. The actual particle height is then used to initiate the following trajectory run step.

For small Reynolds numbers $Re < 0.1$, the terminal velocity can be approximated by the Stokes settling velocity, u_{St}:

$$u_{St} = \frac{D^2 \rho_p g C_c}{18\mu},$$

where D is the particle diameter (μm), which is randomly chosen before starting the trajectory from a Gamma distribution with the probability density function maximized at 2 μm and a mean particle size of 4 μm, namely, $D \sim$ Gamma (shape parameter $k = 2.0$; scale parameter $\theta = 2.0$). Furthermore, ρ_p is the dust particle density, 2.5×10^3 kg m^{-3}; g is the gravitational acceleration, 9.8 m s^{-2}; C_c is the Cunningham slip correction factor, calculated by $C_c = 1 + 0.67/D$, with D in micrometers; and μ is the dynamic viscosity of air, 1.8×10^{-5} kg m^{-1} s^{-1}. The applied particle size distribution is derived from previous observational studies for North Africa (Chou et al., 2008; Kok et al., 2017; Todd et al., 2007).

The applied trajectory modeling also includes wet deposition, which takes into account scavenging of dust particles by water within and beneath observed precipitating clouds. At each trajectory time step, if precipitation is reported to occur and the dust particle, after considering gravitational settling, is located below the cloud top height, then this dust particle is removed, thereby terminating its trajectory. Given the inhomogeneous nature of cloud cover in any satellite pixel, the dust particles in and underneath the precipitating clouds are removed with a probability that is proportional to the pixel's cloud cover fraction. In order to account for the incomplete removal of dust in or underneath precipitating clouds, a removal rate of 80% is further superimposed onto the observed cloud cover fraction, thereby determining the removal probability of dust particles in a specific pixel. The simulated dust transport and deposition are relatively insensitive to the removal rate, based on additional tests using rates ranging from 50% to 100%. Precipitation within 50°S to 50°N is obtained from the 3-hourly, Version 7 Tropical Rainfall Measuring Mission (TRMM) Multi-Satellite Precipitation Analysis (TMPA) at a 0.25° × 0.25° resolution (Huffman et al., 2007). Cloud top height and cloud fraction at a 0.1° × 0.1° resolution are retrieved from the Advanced Very High Resolution Radiometer (AVHRR) Pathfinder Atmospheres-Extended (PATMOS-x) cloud properties data set (Heidinger et al., 2014).

2.3. Quantification of Dust Deposition Fluxes and Dust Mass Loadings From Trajectory Statistics

In order to facilitate the validation and interpretation of the current trajectory analysis, here we convert the trajectory statistics, namely, the number of passing trajectories and terminating trajectories, to dust mass loading and dust deposition fluxes, using in situ observations of dust deposition from 20 sites across the tropical Atlantic Ocean (compiled by H. Yu, Tan, et al., 2019; Table S1). We assume that the total number of terminating trajectories from both North African sources during both winter and summer is proportional to the annual mean dust deposition flux at each pixel with a spatially homogeneous conversion coefficient *Rc*. *Rc* is obtained by regressing the in situ observations of dust deposition flux over the tropical and subtropical Atlantic Ocean upon the collocated number of terminating trajectories. The total dust deposition flux from both North African sources according to the trajectory analysis is subsequently determined (Figure 1). Seasonal dust deposition from either North African sources in boreal winter and summer is determined by multiplying $1.2 \times Rc$ by the corresponding number of terminating trajectories, assuming that wintertime and summertime dust deposition fluxes are 1.5 times of those in spring and autumn, according to H. Yu, Tan, et al. (2019). In order to determine dust mass loading from the current trajectory analysis, dust loss fraction (LF) is computed to reflect the spatial distribution of dust removal efficiency. Dust LF (day^{-1}) at each pixel is calculated as the ratio between the total number of terminating trajectories and total number of passing trajectories from both North African sources in both boreal winter and summer. This approach results in a regional average LF of about 0.1 over the tropical and subtropical Atlantic Ocean, consistent with estimates from multiple satellite observations (H. Yu, Tan, et al., 2019). Dust mass loading from each North African dust source in each season is subsequently calculated by dividing the currently derived seasonal, source-specific dust deposition flux by LF at each pixel.

The spatial distribution of annual mean dust deposition from in situ measurements and the total number of terminating trajectories from the leading two North African dust sources are largely consistent (Figure 1). The correlation of 0.77 between the two metrics demonstrates confidence in the current assumption that the total number of terminating trajectories from both North African sources in both winter and summer

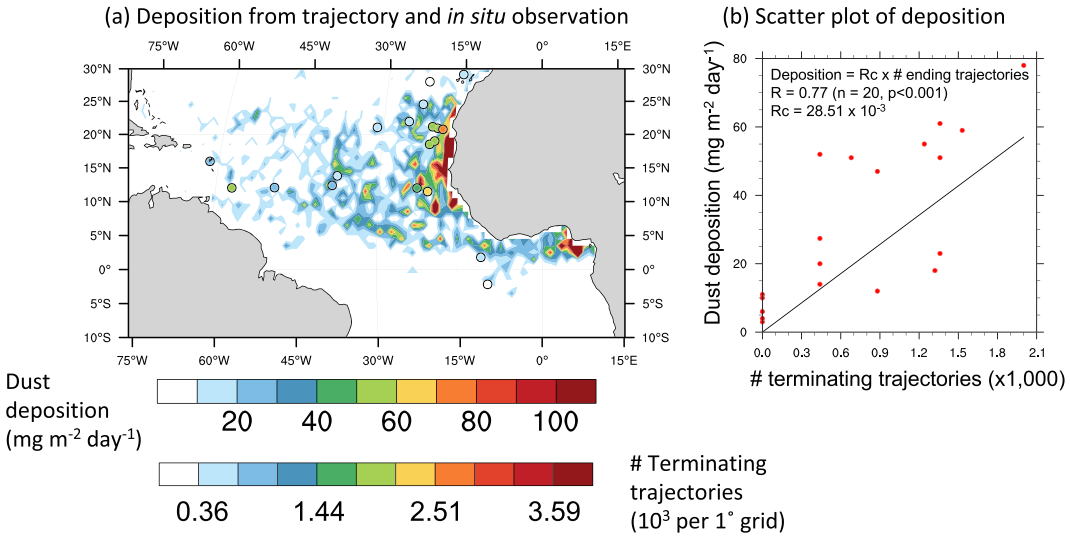

Figure 1. Quantification of dust deposition fluxes based on the current trajectory statistics and in situ observations. (a) Total number of trajectories terminating in each 1° × 1° pixel from both North African sources in both JFM and JJA and in situ observations of annual mean dust deposition flux (mg m^{-2} day^{-1}) across the tropical Atlantic Ocean. (b) Scatterplot of dust deposition and collocated number of terminating trajectories. *Rc* denotes the slope of the regression line.

is proportional to the annual mean dust deposition flux at each pixel. The imperfect linear relationship between in situ dust deposition and the number of terminating trajectories can be largely attributed to the different temporal coverage of in situ observations and the current trajectory analysis.

2.4. Validation of the Trajectory-Based Dust Loading

In order to validate the current trajectory analysis against satellite observations, dust AOD (DAOD) and dust extinction are further calculated from trajectory-based dust loading using mass extinction efficiency (MEE). Following H. Yu, Tan, et al. (2019), MEE is a linear function of longitude across the tropical and subtropical Atlantic Ocean, decreasing from 0.60 m^2 g^{-1} at 100°W to 0.37 m^2 g^{-1} at 20°W. DAOD or dust extinction is calculated by multiplying MEE with column dust mass loading or dust mass concentration.

Version 23, Level 2 MISR 550-nm nonspherical, DAOD at 4.4-km resolution (Garay et al., 2020) is used to validate the horizontal distribution of dust loading assessed by the current trajectory analysis. The MISR nonspherical AOD fraction is often referred to as "fraction of total AOD due to dust," as dust is the primary nonspherical aerosol particle in the atmosphere, especially over desert regions such as those found in North Africa (Kalashnikova et al., 2005). In addition to MISR DAOD, MODIS 550-nm DAOD is also used to validate the longitudinal distribution of dust loading obtained from the current trajectory analysis. MODIS DAOD is calculated from AOD and fine mode fraction (Remer et al., 2005) in the Dark Target retrieval product, following the approach described by H. Yu, Tan, et al. (2019). Dust extinction profile at 532 nm from the Cloud-Aerosol Lidar with Orthogonal Polarization (CALIOP) Version 4.10 (V4) Level 2 aerosol data products (M. H. Kim et al., 2018) is used to validate the vertical distribution of dust loading obtained from the current trajectory analysis. In this study, we use both daytime and nighttime, clear sky aerosol extinction for "dust" and dust mixtures, namely, "polluted dust" and "dusty marine."

3. Results

3.1. Validation of the Trajectory-Based Dust Loading

The seasonal dust loading from the leading two North African dust sources, based on the current study's trajectory simulations, resembles the MISR DAOD field over the tropical Atlantic Ocean (Figures 2a and 2b), thereby validating the applied trajectory simulations. The overall dust loading contributed by both North African sources has a spatial correlation of 0.79 and 0.76 (n = 2,351 oceanic grid cells in 10°S to 30°N, 75°W to 15°E, both p values <0.001) with the MISR DAOD in boreal winter (JFM) and summer (JJA), respectively. The overall dust loading from the two North African dust sources also captures the

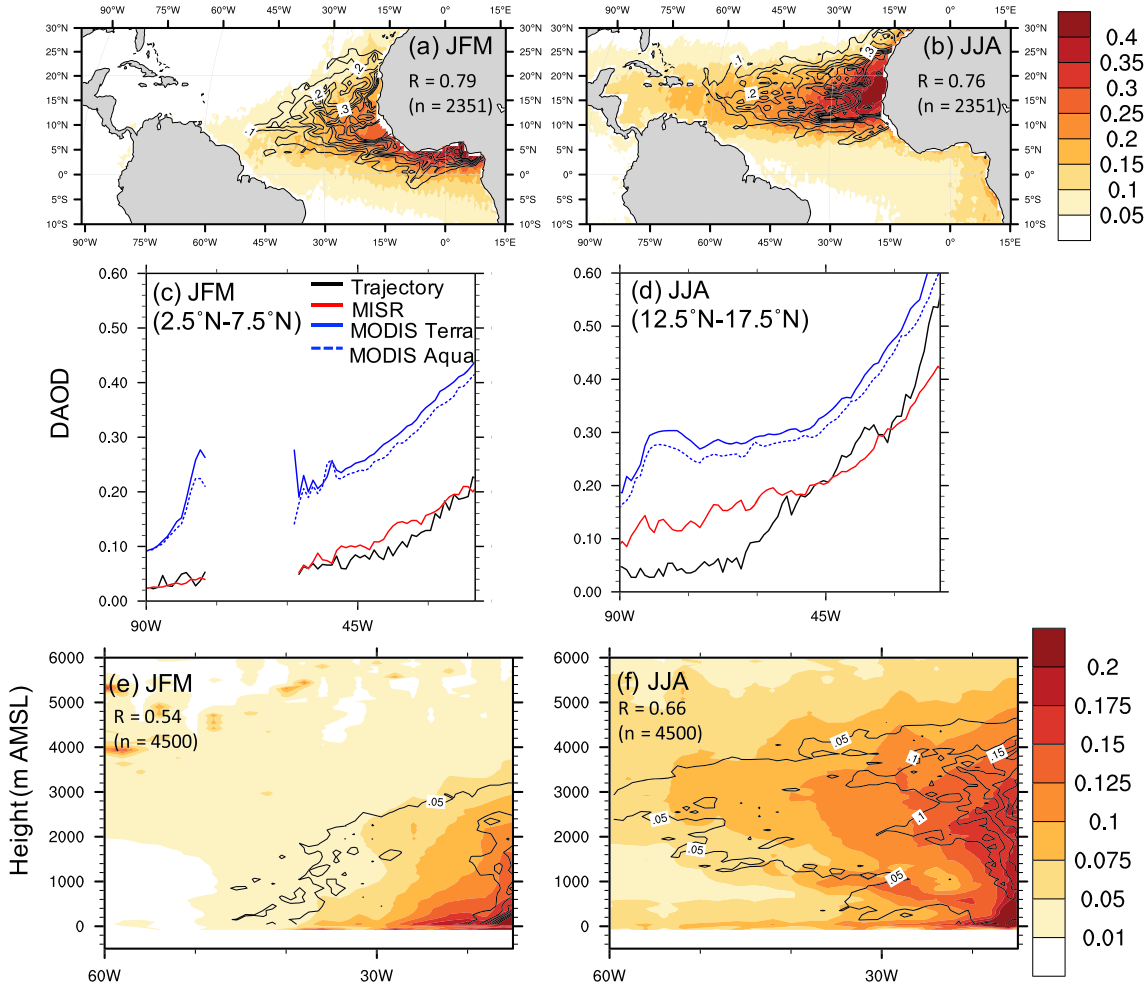

Figure 2. Comparison of dust loading between the current trajectory analysis and satellite observations. (a, b) DAOD from the current trajectory analysis (contour), contributed by both North African dust sources, and MISR (color) during (a) JFM and (b) JJA 2005–2017. (c, d) Seasonally and zonally averaged DAOD from the current trajectory analysis (black), MISR (red), MODIS on Terra (blue solid), and MODIS on Aqua (blue dashed) in (a) JFM, across 2.5°N to 7.5°N, and (b) JJA, across 12.5°N to 17.5°N, during 2005–2017. (e, f) Dust extinction coefficient from the current trajectory analysis (contour), contributed by both North African dust sources, and CALIOP (color) between 5°N and 25°N by altitude (m AMSL) and longitude during 2006–2017 in (c) JFM and (d) JJA. The spatial correlation between the observational and trajectory-based DAOD or dust extinction fields is denoted on the corresponding panel.

longitudinal distribution of MISR and MODIS DAOD over the tropical Atlantic Ocean (Figures 2c and 2d). Although the current trajectory analysis produces lower DAOD than observations from MISR and MODIS over the western tropical Atlantic Ocean in boreal summer, the relative bias is substantially reduced from the GOCART model (D. Kim et al., 2017).

According to the comparison between the overall trajectory-based and observed seasonal dust concentration profiles from CALIOP (Figures 2e and 2f), the current study's trajectory simulations demonstrate moderate skill in capturing the vertical distribution of dust particles from the west coast of North Africa to the western tropical Atlantic Ocean. The majority of dust particles from the leading two North African dust sources are present between the surface and 2 km above mean sea level (AMSL) during boreal winter and 4 km AMSL during boreal summer over the ocean, reflecting the typical vertical structure of the SAL and its seasonal variability (Kuciauskas et al., 2018; Prospero & Carlson, 1972, 1980). The inclusion of dry and wet depositions is key to accurately constraining the vertical distribution of dust particles along their transatlantic transport from both sources (Figure S1). During both boreal winter and summer, the majority of elevated dust particles are removed by wet deposition within or underneath precipitating clouds. During boreal summer, wet deposition is particularly responsible for reducing the presence of dust particles underneath the typical cloud top (3–4 km AMSL) over the tropical Atlantic Ocean.

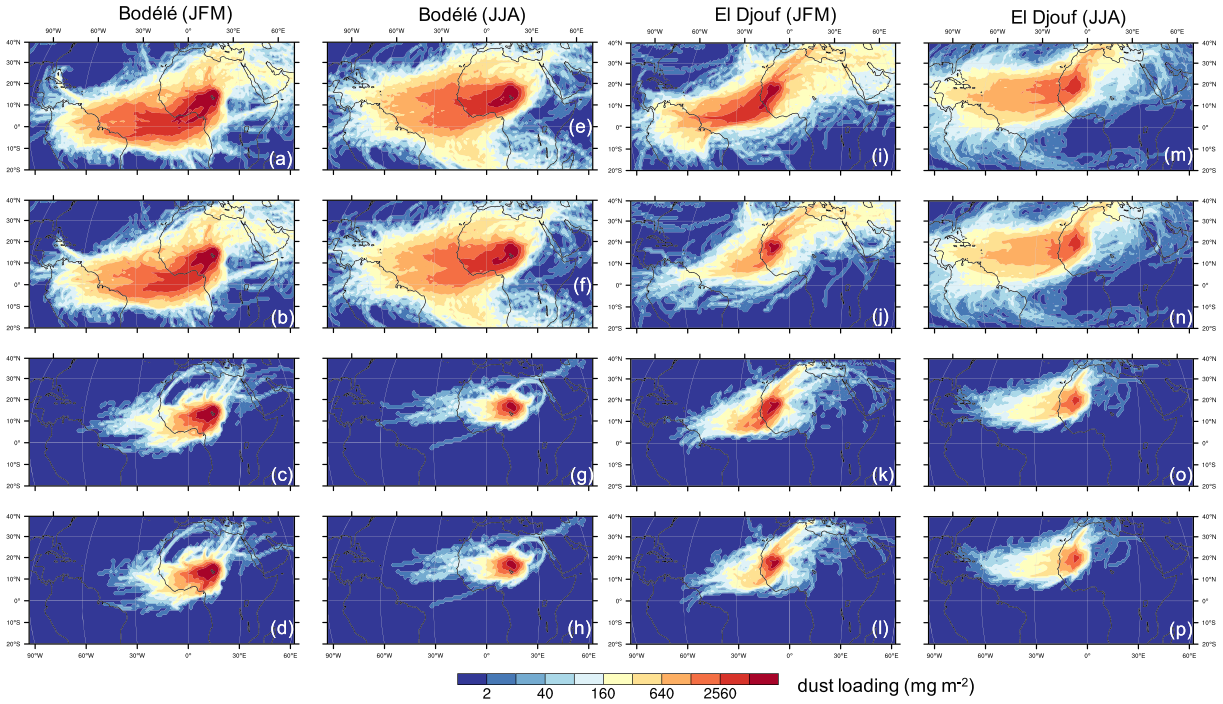

Figure 3. Spatial distribution of dust loading (mg m^{-2}) contributed by dust emission from the (a–h) Bodélé depression and (i–p) El Djouf during (a–d, i–l) January–March (JFM) and (e–h and m–p) June–August (JJA) in 2005–2017. In (a), (e), (i), and (m), neither wet nor dry deposition is considered; in (b), (f), (j), and (n), only dry deposition is considered; in (c), (g), (k), and (o), only wet deposition is considered; and in (d), (h), (l), and (p), both dry and wet deposition are considered.

3.2. Dust Transport and Deposition From the El Djouf and Bodélé Depression

According to trajectory simulations that account for both dry and wet deposition, the El Djouf is the dominant source of North African dust transport to the Amazon Basin and Caribbean Sea, during boreal winter and summer, respectively, rather than the Bodélé depression (Figures 3 and 4). During boreal winter, dust particles from the El Djouf are transported southwestward to the tropical Atlantic Ocean (Figure 3) and

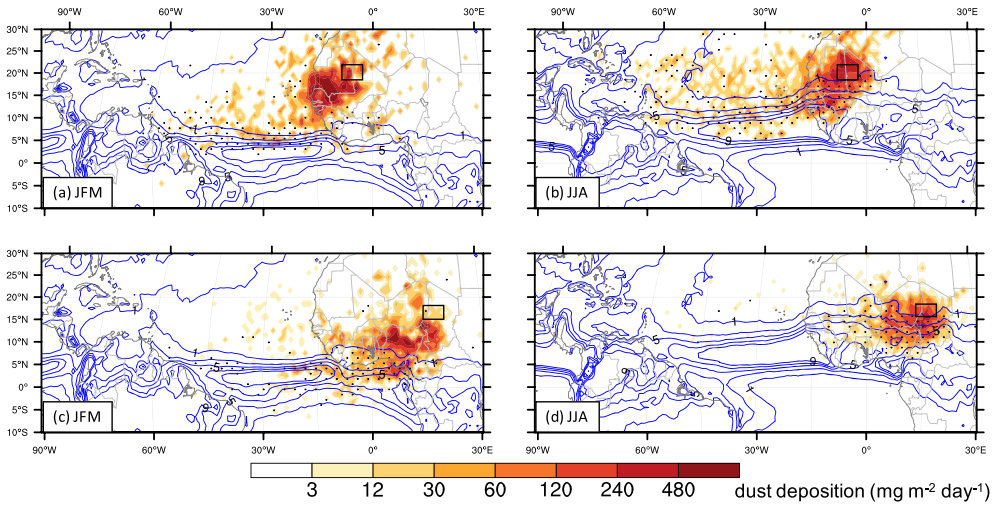

Figure 4. Dust deposition (mg m^{-2} day^{-1}) after emission from the (a, b) El Djouf and (c, d) Bodélé depression in (a, c) JFM and (b, d) JJA during 2005–2017. The shading represents the total combined wet and dry deposition. The stitches indicate areas where wet deposition dominates, exceeding 70% of the total dust deposition in that pixel. Blue contours indicate the seasonally averaged precipitation (mm day^{-1}) from TMPA during 2005–2017.

largely removed by substantial rainfall around 5°N associated with the northern flank of the Intertropical Convergence Zone (ITCZ) (Ashpole & Washington, 2013; Janicot et al., 2011; Nicholson, 2009); 61.2 Tg season^{-1} (52.8–70.4 among trajectory subsamples) and 3.6 Tg season^{-1} (0.6–5.6) of the dust particles are deposited over the tropical Atlantic Ocean and Amazon Basin, respectively (Figure 4a). During boreal summer, a relatively large portion of dust particles from the El Djouf are transported westward by the African easterly jet to the tropical Atlantic Ocean around 15°N (Cook, 1999; Knippertz & Todd, 2012). Given the typical location of the ITCZ around 10°N during boreal summer (Ashpole & Washington, 2013; Janicot et al., 2011), 4.9 Tg season^{-1} (2.1–6.8) of dust particles from the El Djouf is eventually deposited over the Caribbean Sea with strong cloud scavenging in JJA (Figure 4b).

In contrast to West African dust transport, the majority of dust particles from the Bodélé depression are removed over land, primarily by gravitational settling during boreal winter and intense precipitation associated with the intertropical rain belt during boreal summer (Nicholson, 2009). Although 20.9 Tg season^{-1} (14–26.8) of dust particles from the Bodélé depression is transported southwestward to the Gulf of Guinea during boreal winter (Figure 3c), they are mostly removed by intense rainfall associated with ITCZ, resulting in only 0.4 Tg season^{-1} (0–0.8) of dust from the Bodélé depression eventually depositing over the Amazon Basin during boreal winter (Figure 4c). The extensive near-source dust removal primarily by dry deposition during boreal winter and wet deposition during boreal summer, as identified by the current trajectory analysis (Figures 4c and 4d), is supported by the observed evolution of dust vertical structures near the Bodélé depression (Figure S2). Given the similar amount of dust being lifted per event from the El Djouf and Bodélé depression during boreal winter, as represented by the MISR DAOD of 0.21 $\pm$ 0.19 (mean $\pm$ one standard deviation) over the Bodélé depression and 0.19 $\pm$ 0.17 over the El Djouf (Figure S3), the El Djouf clearly dominates over the Bodélé depression in terms of dust transport contribution to the Amazon Basin in boreal winter and spring. During boreal summer, the El Djouf is the preferred dust source to the tropical Atlantic and Caribbean Islands, attributed to both higher amount of dust emission (Figure S3) and favorable dust transport pathways, compared with the Bodélé depression, consistent with geochemical evidence (Bozlaker et al., 2018; Kumar et al., 2018; Pourmand et al., 2014).

Based on the current trajectory simulations, the relative contributions from the Bodélé depression and El Djouf are primarily determined by the distinct transport pathways and interaction with seasonal rain belts. If neither dry nor wet deposition is considered during the trajectory analysis, the Bodélé depression appears to contribute substantially to dust transport to the Amazon Basin, with a total of 20.5 Tg season^{-1} (16.2–24.8) of the dust particles released from the Bodélé depression passing over the Amazon Basin within 14 days in JFM (Figures 3a and 3e), which is comparable to the contribution from the El Djouf (Figures 3i and 3m). However, by considering transport pathways with respect to the position of seasonal rain belts, as well as the climatologically stronger atmospheric subsidence (Figure S4) that supports more substantial dry deposition near the dust source, dust particles released from the Bodélé depression are more vulnerable to dry and wet deposition, compared with dust from the El Djouf (Figure 4).

4. Conclusions and Discussion

The current study, through an examination of a suite of satellite observations under an observation-constrained trajectory analysis framework, presents observation-derived evidence that the El Djouf dominantly provides dust for transatlantic transport from North Africa to the Americas. According to this observation-constrained quantification of wet deposition, dust particles from both the Bodélé depression and El Djouf are predominantly removed by water within and underneath precipitating clouds associated with the ITCZ over ocean and intertropical rain belts over land. However, the transport pathways of dust released over the El Djouf are less affected by the seasonal rainy clouds than those associated with the Bodélé depression, thereby leading to greater contribution from the former region to transatlantic dust transport to the Americas. Furthermore, the current quantification of wet deposition provides useful observational constraints for CTMs, supplementing in situ dust records in the Caribbean at Barbados (Prospero & Mayol-Bracero, 2013), in South America at Cayenne, French Guiana (Barkley et al., 2019; Prospero et al., 2014, 1981), and at the Amazon Tall Tower Observatory (ATTO) (Saturno et al., 2018; Val Martin et al., 2010).

Based on a large ensemble of observationally constrained trajectory simulations, the present study indicates that the Bodélé depression contributes little to transatlantic dust transport and dust deposition over the Amazon Rainforest in boreal winter and spring, in clear disagreement with prior studies' findings based on AOD-based dust flux calculations (Kaufman et al., 2005; Koren et al., 2006). As pointed out by H. Yu, Chin, Yuan, et al. (2015), these earlier efforts (Kaufman et al., 2005; Koren et al., 2006) were subject to inaccurate geographic definition of the Amazon Basin and exclusion of meridional dust transport. In addition, the current advanced trajectory simulations challenge two key assumptions underlying the AOD-based dust flux calculation by Koren et al. (2006), namely, that (1) dust aerosols over the broad downwind region (0–20°N, 0–20°E) all originate from the Bodélé depression and (2) deposition rates over West Africa are similar to those over the tropical Atlantic Ocean.

In addition, uncertainties in the satellite AOD and dust loading retrievals need to be accounted for in satellite-based dust flux calculations. AOD-based dust flux calculations near the source region are likely to be biased low because extremely dense dust plumes, typically present over dust source regions, often lead to the failure of MISR and MODIS AOD retrievals at AODs above 3 (Witek et al., 2018). For example, apparently higher AOD over the downwind region than over the Bodélé depression itself is present in MISR observations, as extremely dense dust layers over the Bodélé depression cause AOD retrieval failure and reported missing values (Figure S5). In another example, we know that the laser backscatter signal becomes totally attenuated at particulate column optical depths of about 3, so that there are occasions where CALIOP cannot measure the full extent of the vertical column in the thick dust layer (Vaughan et al., 2009). This complete attenuation problem likely leads to underestimation of the near-surface dust extinction by CALIOP over both the El Djouf and Bodélé depression. The aforementioned issues in satellite observations of AOD or dust loading should be added to the reported 45–70% uncertainty in the CALIOP-based dust flux estimation (H. Yu, Chin, Bian, et al., 2015; H. Yu, Chin, Yuan, et al., 2015).

Indeed, the aforementioned uncertainties in the satellite AOD and dust loading retrievals also lead to a limitation in the current trajectory analysis framework. Ideally, the number of particles released from each dust plume should be proportional to the dust mass loading at dust sources. However, due to the lack of credible AOD or dust loading retrievals over dust sources, the initial mass loading at dust sources is hard to determine, leading us to base the trajectory initializations on assumptions that are difficult to test at the source. The proof of the accuracy of these assumptions is the reasonable consistency in dust deposition and loading obtained between the current trajectory analysis and satellite observations (Figure 2). It is this consistency that provides confidence in the credibility of the current study's conclusions.

Other sources of uncertainty in the current study include the limited temporal coverage and spatial resolution of satellite observations, as well as mixing of dust and biomass burning aerosols during transport. For example, due to the diurnal variability in dust activation over the two deserts, MISR overpass in the morning leads to underrepresentation of dust activation during the rest of the day. Over the Bodélé depression, where dust activity associated with high surface wind speeds peaks in the morning with the breakdown of the nocturnal low-level jet (Schepanski et al., 2015; Washington & Todd, 2005), MISR is very likely to capture the majority of dust activation events. Over the El Djouf, in addition to the morning dust activation driven by the breakdown of the nocturnal low-level jet, a portion of dust storms is also caused by strong downbursts associated with afternoon deep convection (Fiedler et al., 2013; Heinold et al., 2013). Furthermore, biomass burning aerosols are likely mixed with dust aerosols during the transport of Bodélé dust over western Sahel and central Africa (Adams et al., 2012; Ansmann et al., 2009; Barkley et al., 2019). The dust-smoke mixing produces larger particles that are easier for gravitational settling, thereby resulting in even fewer dust particles from the Bodélé depression to affect the Amazon Basin. Considering the diurnal variability in dust activation and mixing of dust and smoke along transport, we hypothesize that the actual contribution of the El Djouf to transatlantic dust transport further overwhelms the contribution from the Bodélé depression.

Data Availability Statement

Data sets for this research are included in this paper and in the supporting information. MISR CMVP and DAOD data are available through Garay et al. (2020) and Y. Yu et al. (2018). CALIOP dust extinction data are available through M. H. Kim et al. (2018).

Acknowledgments

This work was partially performed at the Jet Propulsion Laboratory, California Institute of Technology, under a contract with the National Aeronautics and Space Administration. The effort of Dr. Michael Notaro was supported by the U.S. Department of Energy (DOE) (Grant DE-SC0012534) Regional and Global Climate Modeling (RGCM) program. The authors thank the MISR team for providing facilities and useful discussions. The comments from Dr. Lorraine Remer and an anonymous reviewer were greatly appreciated.

References

Abouchami, W., Näthe, K., Kumar, A., Galer, S. J. G., Jochum, K. P., Williams, E., et al. (2013). Geochemical and isotopic characterization of the Bodélé depression dust source and implications for transatlantic dust transport to the Amazon basin. *Earth and Planetary Science Letters*, *380*, 112–123. https://doi.org/10.1016/j.epsl.2013.08.028

Adams, A. M., Prospero, J. M., & Zhang, C. (2012). CALIPSO-derived three-dimensional structure of aerosol over the Atlantic basin and adjacent continents. *Journal of Climate*, *25*(19), 6862–6879. https://doi.org/10.1175/JCLI-D-11-00672.1

Ansmann, A., Baars, H., Tesche, M., Müller, D., Althausen, D., Engelmann, R., et al. (2009). Dust and smoke transport from Africa to South America: Lidar profiling over Cape Verde and the Amazon rainforest. *Geophysical Research Letters*, *36*, L11802. https://doi.org/10.1029/2009GL037923

Ashpole, I., & Washington, R. (2013). Intraseasonal variability and atmospheric controls on daily dust occurrence over the central and western Sahara. *Journal of Geophysical Research: Atmospheres*, *118*, 915–926. https://doi.org/10.1002/2013JD020267

Barkley, A. E., Prospero, J. M., Mahowald, N., Hamilton, D. S., Popendorf, K. J., Oehlert, A. M., et al. (2019). African biomass burning is a substantial source of phosphorus deposition to the Amazon, Tropical Atlantic Ocean, and Southern Ocean. *Proceedings of the National Academy of Sciences of the United States of America*, *116*(33), 16216–16221. https://doi.org/10.1073/pnas.1906091116

Ben-Ami, Y., Koren, I., & Altaratz, O. (2009). Patterns of North African dust transport over the Atlantic: Winter vs. summer, based on CALIPSO first year data. *Atmospheric Chemistry and Physics*, *9*(20), 7867–7875. https://doi.org/10.5194/acp-9-7867-2009

Ben-Ami, Y., Koren, I., Rudich, Y., Artaxo, P., Martin, S. T., & Andreae, M. O. (2010). Transport of North African dust from the Bodélé depression to the Amazon Basin: A case study. *Atmospheric Chemistry and Physics*, *10*(16), 7533–7544. https://doi.org/10.5194/acp-10-7533-2010

Bozlaker, A., Prospero, J. M., Price, J., & Chellam, S. (2018). Linking Barbados mineral dust aerosols to North African sources using elemental composition and radiogenic Sr, Nd, and Pb isotope signatures. *Journal of Geophysical Research: Atmospheres*, *123*, 1384–1400. https://doi.org/10.1002/2017JD027505

Bristow, C. S., Hudson-Edwards, K. A., & Chappell, A. (2010). Fertilizing the Amazon and equatorial Atlantic with West African dust. *Geophysical Research Letters*, *37*, L14807. https://doi.org/10.1029/2010GL043486

Chomette, O., Legrand, M., & Marticorena, B. (1999). Determination of the wind speed threshold for the emission of desert dust using satellite remote sensing in the thermal infrared. *Journal of Geophysical Research*, *104*(D24), 31,207–31,215. https://doi.org/10.1029/1999JD900756

Chou, C., Formenti, P., Maille, M., Ausset, P., Helas, G., Harrison, M., & Osborne, S. (2008). Size distribution, shape, and composition of mineral dust aerosols collected during the African Monsoon Multidisciplinary Analysis Special Observation Period 0: Dust and Biomass-Burning Experiment field campaign in Niger, January 2006. *Journal of Geophysical Research*, *113*, D00C10. https://doi.org/10.1029/2008JD009897

Cook, K. H. (1999). Generation of the African easterly jet and its role in determining West African precipitation. *Journal of Climate*, *12*(5), 1165–1184. https://doi.org/10.1175/1520-0442(1999)012<1165:GOTAEJ>2.0.CO;2

Crouvi, O., Schepanski, K., Amit, R., Gillespie, A. R., & Enzel, Y. (2012). Multiple dust sources in the Sahara Desert: The importance of sand dunes. *Geophysical Research Letters*, *39*, L13401. https://doi.org/10.1029/2012GL052145

Diner, D. J., Beckert, J. C., Reilly, T. H., Bruegge, C. J., Conel, J. E., Kahn, R. A., et al. (1998). Multi-angle Imaging SpectroRadiometer (MISR) instrument description and experiment overview. *IEEE Transactions on Geoscience and Remote Sensing*, *36*, 1072–1087. https://doi.org/10.1109/36.700992

Evan, A. T., Flamant, C., Gaetani, M., & Guichard, F. (2016). The past, present and future of African dust. *Nature*, *531*(7595), 493–495. https://doi.org/10.1038/nature17149

Fiedler, S., Schepanski, K., Heinold, B., Knippertz, P., & Tegen, I. (2013). Climatology of nocturnal low-level jets over North Africa and implications for modeling mineral dust emission. *Journal of Geophysical Research: Atmospheres*, *118*, 6100–6121. https://doi.org/10.1002/jgrd.50394

Garay, M. J., Witek, M. L., Kahn, R. A., Seidel, F. C., Limbacher, J. A., Bull, M. A., et al. (2020). Introducing the 4.4 km spatial resolution Multi-Angle Imaging SpectroRadiometer (MISR) aerosol product. *Atmospheric Measurement Techniques*, *13*(2), 593–628. https://doi.org/10.5194/amt-13-593-2020

Ginoux, P., Chin, M., Tegen, I., Prospero, J. M., Holben, B., Dubovik, O., & Lin, S.-J. (2001). Sources and distributions of dust aerosols simulated with the GOCART model. *Journal of Geophysical Research*, *106*(D17), 20,255–20,273. https://doi.org/10.1029/2000JD000053

Ginoux, P., Garbuzov, D., & Hsu, N. C. (2010). Identification of anthropogenic and natural dust sources using Moderate Resolution Imaging Spectroradiometer (MODIS) Deep Blue level 2 data. *Journal of Geophysical Research*, *115*, D05204. https://doi.org/10.1029/2009JD012398

Ginoux, P., Prospero, J. M., Gill, T. E., Hsu, N. C., & Zhao, M. (2012). Global-scale attribution of anthropogenic and natural dust sources and their emission rates based on MODIS Deep Blue aerosol products. *Reviews of Geophysics*, *50*, RG3005. https://doi.org/10.1029/2012RG000388

Gläser, G., Wernli, H., Kerkweg, A., & Teubler, F. (2015). The transatlantic dust transport from North Africa to the Americas—Its characteristics and source regions. *Journal of Geophysical Research: Atmospheres*, *120*, 11,231–11,252. https://doi.org/10.1002/2015JD023792

Heidinger, A. K., Foster, M. J., Walther, A., & Zhao, X. (2014). The Pathfinder Atmospheres-Extended AVHRR climate dataset. *Bulletin of the American Meteorological Society*, *95*, 909–922. https://doi.org/10.1175/BAMS-D-12-00246.1:Atmospheres

Heinold, B., Knippertz, P., Marsham, J. H., Fiedler, S., Dixon, N. S., Schepanski, K., et al. (2013). The role of deep convection and nocturnal low-level jets for dust emission in summertime West Africa: Estimates from convection-permitting simulations. *Journal of Geophysical Research: Atmospheres*, *118*, 4385–4400. https://doi.org/10.1002/jgrd.50402

Hudson-Edwards, K. A., Bristow, C. S., Cibin, G., Mason, G., & Peacock, C. L. (2014). Solid-phase phosphorus speciation in Saharan Bodélé Depression dusts and source sediments. *Chemical Geology*, *384*, 16–26. https://doi.org/10.1016/j.chemgeo.2014.06.014

Huffman, G. J., Bolvin, D. T., Nelkin, E. J., Wolff, D. B., Adler, R. F., Gu, G., et al. (2007). The TRMM Multisatellite Precipitation Analysis (TMPA): Quasi-global, multiyear, combined-sensor precipitation estimates at fine scales. *Journal of Hydrometeorology*, *8*(1), 38–55. https://doi.org/10.1175/JHM560.1

Janicot, S., Caniaux, G., Chauvin, F., de Coëtlogon, G., Fontaine, B., Hall, N., et al. (2011). Intraseasonal variability of the West African monsoon. *Atmospheric Science Letters*, *12*(1), 58–66. https://doi.org/10.1002/asl.280

Kalashnikova, O. V., Kahn, R., Sokolik, I. N., & Li, W.-H. (2005). Ability of multiangle remote sensing observations to identify and distinguish mineral dust types: Optical models and retrievals of optically thick plumes. *Journal of Geophysical Research*, *110*, D18S14. https://doi.org/10.1029/2004jd004550

Kaufman, Y. J., Koren, I., Remer, L. A., Tanré, D., Ginoux, P., & Fan, S. (2005). Dust transport and deposition observed from the Terra-Moderate Resolution Imaging Spectroradiometer (MODIS) spacecraft over the Atlantic Ocean. *Journal of Geophysical Research*, *110*, D10S12. https://doi.org/10.1029/2003JD004436

Kim, D., Chin, M., Remer, L. a., Diehl, T., Bian, H., Yu, H., et al. (2017). Role of surface wind and vegetation cover in multi-decadal variations of dust emission in the Sahara and Sahel. *Atmospheric Environment*, *148*, 282–296. https://doi.org/10.1016/j.atmosenv.2016.10.051

Kim, M. H., Omar, A. H., Tackett, J. L., Vaughan, M. A., Winker, D. M., Trepte, C. R., et al. (2018). The CALIPSO version 4 automated aerosol classification and lidar ratio selection algorithm. *Atmospheric Measurement Techniques*, *11*(11), 6107–6135. https://doi.org/10.5194/amt-11-6107-2018

Knippertz, P., & Todd, M. C. (2012). Mineral dust aerosols over the Sahara: Meteorological controls on emission and transport and implications for modeling. *Reviews of Geophysics*, *50*, RG1007. https://doi.org/10.1029/2011RG000362

Kok, J. F., Zhou, Q., Miller, R. L., Ridley, D. A., Haustein, K., Albani, S., et al. (2017). Smaller desert dust cooling effect estimated from analysis of dust size and abundance. *Nature Geoscience*, *10*(4), 274–278. https://doi.org/10.1038/ngeo2912

Koren, I., Kaufman, Y. J., Washington, R., Todd, M. C., Rudich, Y., Martins, J. V., & Rosenfeld, D. (2006). The Bodélé depression: A single spot in the Sahara that provides most of the mineral dust to the Amazon forest. *Environmental Research Letters*, *1*(1), 014005. https://doi.org/10.1088/1748-9326/1/1/014005

Kuciauskas, A. P., Xian, P., Hyer, E. J., Oyola, M. I., & Campbell, J. R. (2018). Supporting weather forecasters in predicting and monitoring Saharan air layer dust events as they impact the greater Caribbean. *Bulletin of the American Meteorological Society*, *99*(2), 259–268. https://doi.org/10.1175/BAMS-D-16-0212.1

Kumar, A., Abouchami, W., Galer, S. J. G., Singh, S. P., Fomba, K. W., Prospero, J. M., & Andreae, M. O. (2018). Seasonal radiogenic isotopic variability of the African dust outflow to the tropical Atlantic Ocean and across to the Caribbean. *Earth and Planetary Science Letters*, *487*, 94–105. https://doi.org/10.1016/j.epsl.2018.01.025

Menut, L. (2008). Sensitivity of hourly Saharan dust emissions to NCEP and ECMWF modeled wind speed. *Journal of Geophysical Research*, *113*, D16201. https://doi.org/10.1029/2007JD009522

Moroney, C., Davies, R., & Muller, J. P. (2002). Operational retrieval of cloud-top heights using MISR data. *IEEE Transactions on Geoscience and Remote Sensing*, *40*(7), 1532–1540. https://doi.org/10.1109/TGRS.2002.801150

Nicholson, S. E. (2009). A revised picture of the structure of the "monsoon" and land ITCZ over West Africa. *Climate Dynamics*, *32*(7–8), 1155–1171. https://doi.org/10.1007/s00382-008-0514-3

Okin, G. S., Mahowald, N., Chadwick, O. A., & Artaxo, P. (2004). Impact of desert dust on the biogeochemistry of phosphorus in terrestrial ecosystems. *Global Biogeochemical Cycles*, *18*, GB2005. https://doi.org/10.1029/2003GB002145

Pourmand, A., Prospero, J. M., & Sharifi, A. (2014). Geochemical fingerprinting of trans-Atlantic African dust based on radiogenic Sr-Nd-Hf isotopes and rare earth element anomalies. *Geology*, *42*(8), 675–678. https://doi.org/10.1130/G35624.1

Prospero, J. M. (1999). Long-range transport of mineral dust in the global atmosphere: Impact of African dust on the environment of the southeastern United States. *Proceedings of the National Academy of Sciences*, *96*(7), 3396–3403. https://doi.org/10.1073/pnas.96.7.3396

Prospero, J. M., & Carlson, T. N. (1972). Vertical and areal distribution of Saharan dust over the Western equatorial North Atlantic Ocean. *Journal of Geophysical Research*, *77*(27), 5255–5265. https://doi.org/10.1029/JC077i027p05255

Prospero, J. M., & Carlson, T. N. (1980). Saharan air outbreaks over the tropical North Atlantic. *Pure and Applied Geophysics PAGEOPH*, *119*(3), 677–691. https://doi.org/10.1007/BF00878167

Prospero, J. M., Collard, F., Molinié, J., & Jeannot, A. (2014). Characterizing the annual cycle of African dust transport to the Caribbean Basin and South America and its impact on the environment and air quality. *Global Biogeochemical Cycles*, *29*, 757–773. https://doi.org/10.1002/2013GB004802.Received

Prospero, J. M., Glaccum, R. A., & Nees, R. T. (1981). Atmospheric transport of soil dust from Africa to South America. *Nature*, *289*(5798), 570–572. https://doi.org/10.1038/289570a0

Prospero, J. M., & Lamb, P. J. (2003). African droughts and dust transport to the Caribbean: Climate change implications. *Science*, *302*(5647), 1024–1027. https://doi.org/10.1126/science.1089915

Prospero, J. M., & Mayol-Bracero, O. L. (2013). Understanding the transport and impact of African dust on the Caribbean Basin. *Bulletin of the American Meteorological Society*, *94*(9), 1329–1337. https://doi.org/10.1175/BAMS-D-12-00142.1

Remer, L. A., Kaufman, Y. J., Tanré, D., Mattoo, S., Chu, D. A., Martins, J. V., et al. (2005). The MODIS aerosol algorithm, products, and validation. *Journal of the Atmospheric Sciences*, *62*(4), 947–973. https://doi.org/10.1175/JAS3385.1

Ridley, D. A., Heald, C. L., & Ford, B. (2012). North African dust export and deposition: A satellite and model perspective. *Journal of Geophysical Research*, *117*, D02202. https://doi.org/10.1029/2011JD016794

Ridley, D. A., Heald, C. L., Pierce, J. R., & Evans, M. J. (2013). Toward resolution-independent dust emissions in global models: Impacts on the seasonal and spatial distribution of dust. *Geophysical Research Letters*, *40*, 2873–2877. https://doi.org/10.1002/grl.50409

Salvador, P., Alonso-Pérez, S., Pey, J., Artíñano, B., De Bustos, J. J., Alastuey, A., & Querol, X. (2014). African dust outbreaks over the western Mediterranean Basin: 11-year characterization of atmospheric circulation patterns and dust source areas. *Atmospheric Chemistry and Physics*, *14*(13), 6759–6775. https://doi.org/10.5194/acp-14-6759-2014

Saturno, J., Holanda, B. A., Pöhlker, C., Ditas, F., Wang, Q., Moran-Zuloaga, D., et al. (2018). Black and brown carbon over central Amazonia: Long-term aerosol measurements at the ATTO site. *Atmospheric Chemistry and Physics*, *18*(17), 12817–12843. https://doi.org/10.5194/acp-18-12817-2018

Schepanski, K., Knippertz, P., Fiedler, S., Timouk, F., & Demarty, J. (2015). The sensitivity of nocturnal low-level jets and near-surface winds over the Sahel to model resolution, initial conditions and boundary-layer set-up. *Quarterly Journal of the Royal Meteorological Society*, *141*(689), 1442–1456. https://doi.org/10.1002/qj.2453

Schepanski, K., Tegen, I., & Macke, A. (2012). Comparison of satellite based observations of Saharan dust source areas. *Remote Sensing of Environment*, *123*(July 2017), 90–97. https://doi.org/10.1016/j.rse.2012.03.019

Stein, A. F., Draxler, R. R., Rolph, G. D., Stunder, B. J. B., Cohen, M. D., & Ngan, F. (2015). NOAA's HYSPLIT atmospheric transport and dispersion modeling system. *Bulletin of the American Meteorological Society*, *96*(12), 2059–2077. https://doi.org/10.1175/BAMS-D-14-00110.1

Swap, R., Garstang, M., Greco, S., Talbot, R., & Kållberg, P. (1992). Saharan dust in the Amazon Basin. *Tellus*, *44*(2), 133–149. https://doi.org/10.1034/j.1600-0889.1992.t01-1-00005.x

Todd, M. C., Washington, R., Martins, J. V., Dubovik, O., Lizcano, G., M'Bainayel, S., & Engelstaedter, S. (2007). Mineral dust emission from the Bodélé Depression nothern Chad, during BoDEx 2005. *Journal of Geophysical Research*, *112*, D06207. https://doi.org/10.1029/2006JD007170

Val Martin, M., Logan, J. A., Kahn, R. A., Leung, F. Y., Nelson, D. L., & Diner, D. J. (2010). Smoke injection heights from fires in North America: Analysis of 5 years of satellite observations. *Atmospheric Chemistry and Physics*, *10*(4), 1491–1510. https://doi.org/10.5194/acp-10-1491-2010

Vaughan, M. A., Powell, K. A., Kuehn, R. E., Young, S. A., Winker, D. M., Hostetler, C. A., et al. (2009). Fully automated detection of cloud and aerosol layers in the CALIPSO lidar measurements. *Journal of Atmospheric and Oceanic Technology*, *26*(10), 2034–2050. https://doi.org/10.1175/2009JTECHA1228.1

Wang, Q., Saturno, J., Chi, X., Walter, D., Lavric, J. V., Moran-Zuloaga, D., et al. (2016). Modeling investigation of light-absorbing aerosols in the Amazon Basin during the wet season. *Atmospheric Chemistry and Physics*, *16*(22), 14775–14794. https://doi.org/10.5194/acp-16-14775-2016

Washington, R., & Todd, M. C. (2005). Atmospheric controls on mineral dust emission from the Bodélé Depression, Chad: The role of the low level jet. *Geophysical Research Letters*, *32*, L17701. https://doi.org/10.1029/2005GL023597

Washington, R., Todd, M. C., Lizcano, G., Tegen, I., Flamant, C., Koren, I., et al. (2006). Links between topography, wind, deflation, lakes and dust: The case of the Bodélé Depression, Chad. *Geophysical Research Letters*, *33*, L09401. https://doi.org/10.1029/2006GL025827

Witek, M. L., Garay, M. J., Diner, D. J., Bull, M. A., & Seidel, F. C. (2018). New approach to the retrieval of AOD and its uncertainty from MISR observations over dark water. *Atmospheric Measurement Techniques*, *11*(1), 429–439. https://doi.org/10.5194/amt-11-429-2018

Yu, H., Chin, M., Bian, H., Yuan, T., Prospero, J. M., Omar, A. H., et al. (2015). Quantification of trans-Atlantic dust transport from seven-year (2007–2013) record of CALIPSO lidar measurements. *Remote Sensing of Environment*, *159*, 232–249. https://doi.org/10.1016/j.rse.2014.12.010

Yu, H., Chin, M., Yuan, T., Bian, H., Remer, L. a., Prospero, J. M., et al. (2015). The fertilizing role of African dust in the Amazon rainforest: A first multiyear assessment based on data from Cloud-Aerosol Lidar and Infrared Pathfinder Satellite Observations. *Geophysical Research Letters*, *42*, 1984–1991. https://doi.org/10.1002/2015GL063040

Yu, H., Tan, Q., Chin, M., Remer, L. A., Kahn, R. A., Bian, H., et al. (2019). Estimates of African dust deposition along the trans-Atlantic transit using the decadelong record of aerosol measurements from CALIOP, MODIS, MISR, and IASI. *Journal of Geophysical Research: Atmospheres*, *124*, 7975–7996. https://doi.org/10.1029/2019jd030574

Yu, Y., Kalashnikova, O. V., Garay, M. J., Lee, H., & Notaro, M. (2018). Identification and characterization of dust source regions across North Africa and the Middle East using MISR satellite observations. *Geophysical Research Letters*, *45*, 6690–6701. https://doi.org/10.1029/2018GL078324

Yu, Y., Kalashnikova, O. V., Garay, M. J., & Notaro, M. (2019). Climatology of Asian dust activation and transport potential based on MISR satellite observations and trajectory analysis. *Atmospheric Chemistry and Physics*, *19*(1), 363–378. https://doi.org/10.5194/acp-19-363-2019

Zender, C. S. (2003). Mineral Dust Entrainment and Deposition (DEAD) model: Description and 1990s dust climatology. *Journal of Geophysical Research*, *108*(D14), 4416. https://doi.org/10.1029/2002JD002775